Article

Identification of the *Brucea javanica* Constituent Brusatol as a EGFR-Tyrosine Kinase Inhibitor in a Cell-Free Assay

Chonticha Suwattanasophon, Agnes Mistlberger-Reiner, Jon Alberdi-Cedeño, Marc Pignitter, Veronika Somoza, Jürgen König, Thomanai Lamtha, Panatda Wanaragthai, Duangnapa Kiriwan, and Kiattawee Choowongkomon*

ABSTRACT: Inhibitors of the tyrosine kinase (TK) activity of the epidermal growth factor receptor (EGFR) are routinely used in cancer therapy. However, there is a need to discover a new TK inhibitor. This study evaluated extracts from *Brucea javanica* and its components for their potential as novel EGFR-TK inhibitors. The cytotoxic effect of a *g* aqueous extract and its fractions was assessed by MTT assays with A549 lung cancer cells. The two fractions with the highest cytotoxicity were analyzed by LC/MS and ^{1}H NMR. Brusatol was identified as the main constituent of these fractions, and its cytotoxic and pro-apoptotic activities were confirmed in A549 cells. To elucidate the inhibitory activity of brusatol against EGFR-TK, a specific ADP-GloTM kinase assay was used. In this assay, the IC_{50} value for EGFR-TK inhibition was 333.1 nM. Molecular dynamic simulations and docking experiments were performed to identify the binding pocket of brusatol to be located in the intracellular TK-domain of EGFR. This study demonstrates that brusatol inhibits EGFR-TK and therefore harbors a potential as a new therapeutic drug for the therapy of EGFR-depending cancers.
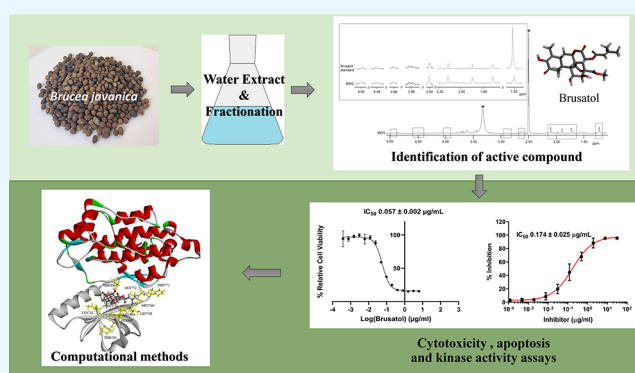
INTRODUCTION

The epidermal growth factor receptor (EGFR) is overexpressed in many cancer types. Activation of EGFR by ligand-binding leads to the activation of the tyrosine kinase (TK) domain, which triggers a signaling cascade which promotes cell growth and cancer survival. Inhibiting the TK activity of EGFR and other receptors is a common approach in cancer therapy, with over 40 compounds approved by the FDA as TK inhibitors for treatment of different cancer types.[1] Despite the great success of the use of TK inhibitors, like afatinib, erlotinib, or gefitinib in lung cancer therapy, the development of resistance to these drugs through mutations, which allow cancer cells to escape the inhibitory effect, is still a major challenge. Therefore, there is a need for the identification of new TK-inhibiting compounds.

Recently, herbal products have become more popular worldwide because it is commonly acknowledged that plants are promising sources for active compounds with potential medical applications. Almost half of the current medicines originate from natural extracts of plants.[2,3] One herbal plant showing medicinal properties is *Brucea javanica* (L.) Merr., a well-known indigenous plant in Southeast Asia and South China,[4] that is used as traditional medicine. In China, *B. javanica* oil (BJO), the oil of the plant's fruit, is administered to

cancer patients in combination with chemotherapy in the form of two patented galenic preparations, i.e., BJO emulsion injection and BJO soft capsule.[5] An extensive meta-analysis on clinical studies applying BJO emulsion injection as an additive to cancer therapy[6] concluded that the BJO emulsion injection enhanced the therapeutic efficacy, especially in digestive system-related cancers, like gastric cancer, and reduced adverse reactions, thus showing a potential for clinical application in cancer therapy. In addition to clinical studies, efforts have been devoted to the elucidation of the chemical composition and the identification of active compounds of *B. javanica* fruits and their specific effects on cancer cells. About 100 chemical constituents have already been reported from this plant, with the majority belonging to the group of quassinoids.[5] Among these, brusatol and bruceine D are the two bioactive compounds, which have been studied most extensively in the context of anti-cancer activity.[5] In vitro as well as in vivo
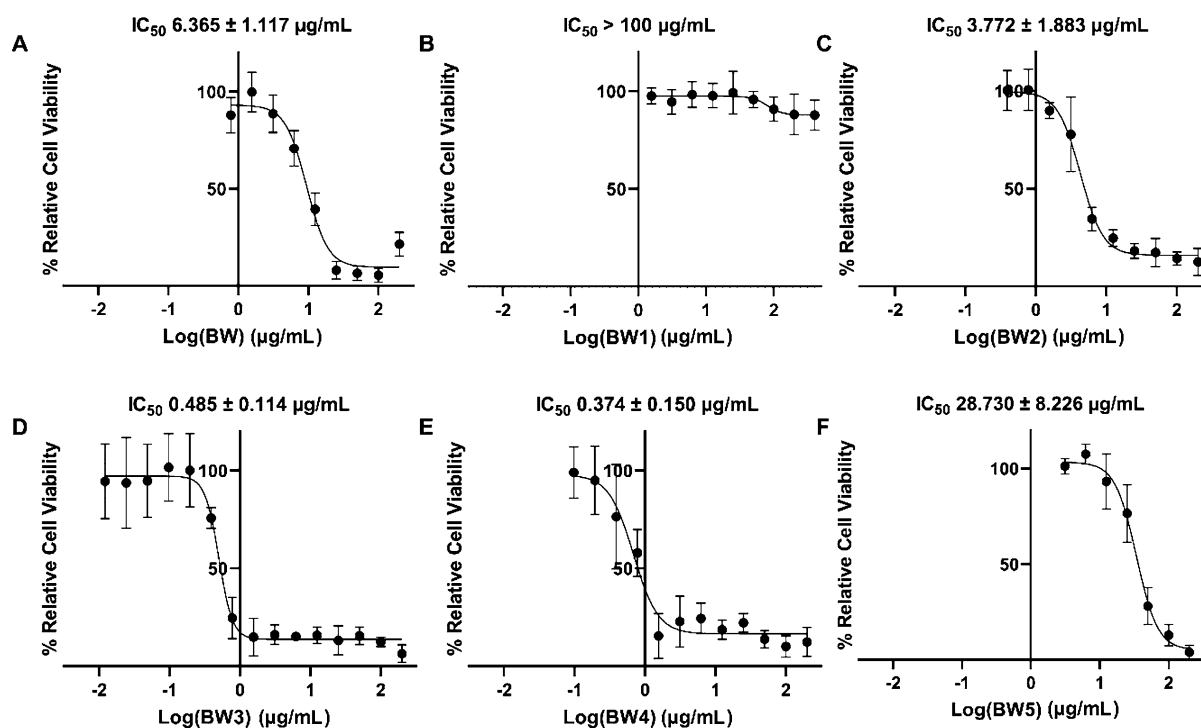
Figure 1. Cytotoxic effect of the *B. javanica* extract and its fractions on A549 cells. The relative cell viability of (A) crude water extract BW, (B) fraction BW1, (C) fraction BW2, (D) fraction BW3, (E) fraction BW4, and (F) fraction BW5 against A549 cancer cells was assessed by MTT assay performed after treatment of A549 cells with the respective sample for 24 h and compared to control cells that were treated with solvent control; results are given as mean ± standard deviation, n = 3 biological and 3 technical replicates each.
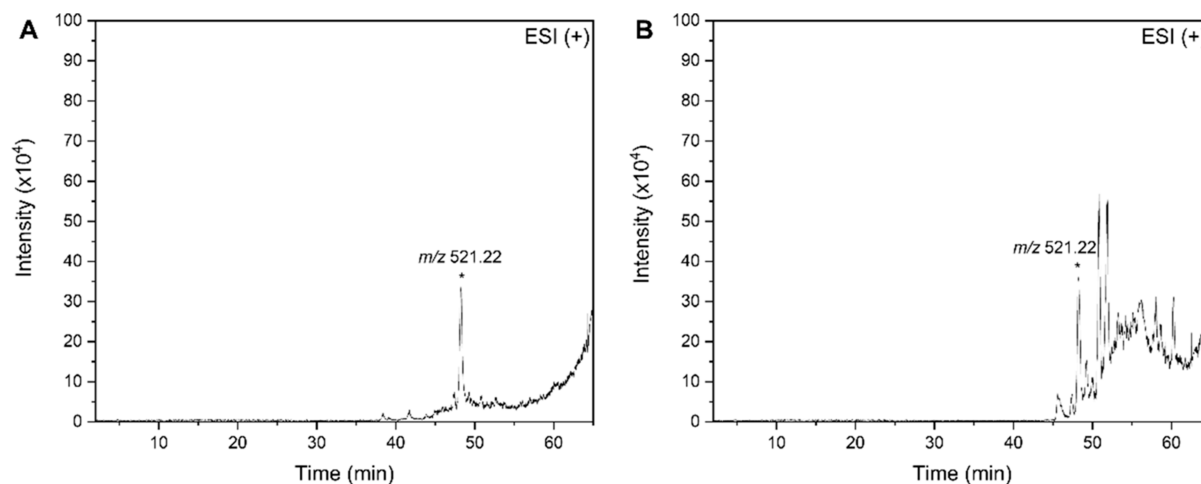
Figure 2. LC/MS analysis of *B. javanica* fractions. Total ion chromatogram of (a) BW3 and (b) BW4 in the positive ionization mode.

studies showed that these compounds and especially brusatol inhibit cellular and tumor growth and other cancer properties in many different cancer types, like lung, colorectal, liver, and pancreatic cancer, via several different pathways, as reviewed by He et al.[7]

Additionally, when screening the extracts of 23 Thai herbs for their EGFR-TK inhibitory activity by using a specific EGFR-TK inhibitory assay,[8] we identified the ethanolic extract of the fruits of *B. javanica* as the second most potent out of the 23 plant extracts. Furthermore, among the tested herb extracts, the *B. javanica* fruit extract had the highest cytotoxic effect on A549 lung cancer cells,[8] which are known to express EGFR and are sensitive to EGFR-TK inhibitors. This leads to the hypothesis that additionally to the already known routes of

anti-cancer activities, constituents of *B. javanica* could also act on cancer cells via EGFR-TK.

The aim of the current study was to identify the active compound from *B. javanica* responsible for the EGFR-TK inhibition and cytotoxicity against lung cancer cells. A549 cells were used as a model system for lung cancer since first-line chemotherapy for this cancer type uses EGFR-TK inhibitors.[1] To reach our aim, an activity-guided fractionation of the extract was performed and complemented with chemical analysis, in vitro assays, and in situ computational analysis.

■ RESULTS AND DISCUSSION

Identification of Cytotoxically Active Fractions of an Aqueous *B. javanica* Extract in A549 Cells. In order to
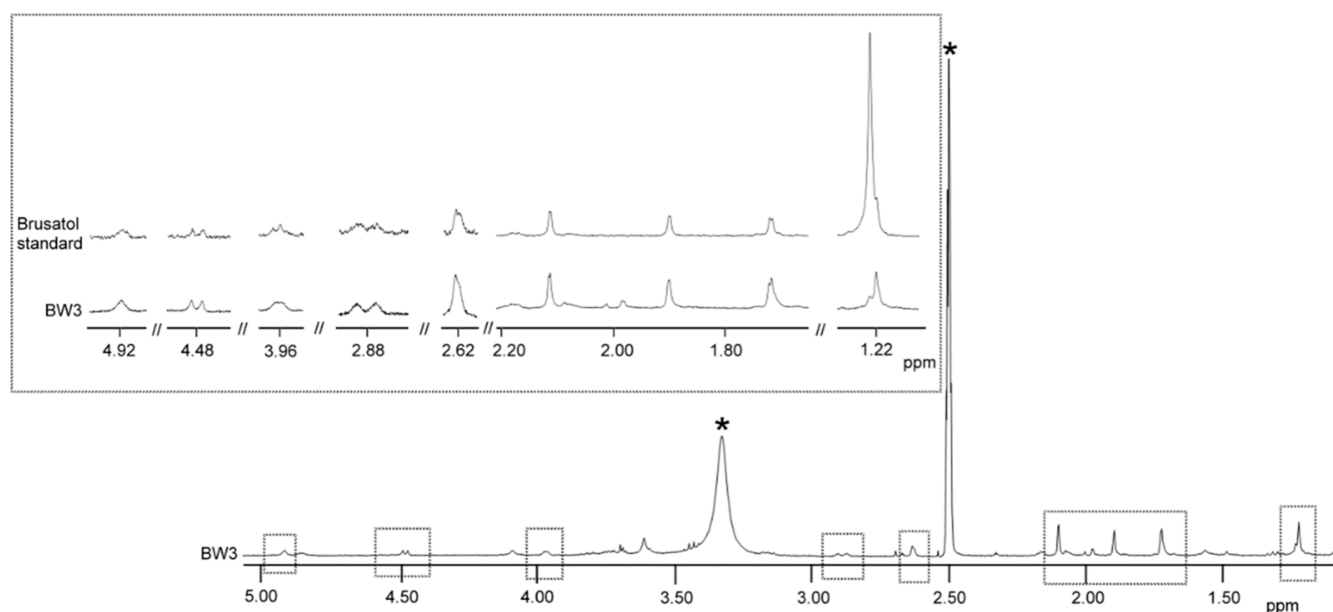
Figure 3. Structural identification of brusatol in *B. javanica* fraction BW3. The full ^{1}H NMR spectrum of BW3 is given, while the insert shows the magnified regions of interest of BW3 in comparison to the same regions within the ^{1}H NMR spectrum of the brusatol standard. Signal marked with * is a satellite peak of DMSO-d_6.

identify the active compound of an aqueous *B. javanica* extract, which has been demonstrated for its EGFR-TK inhibitory activity and cytotoxicity to A549 lung cancer cells,[8] an activity-guided fractionation approach was performed. The cytotoxicity assessment was chosen as a first step toward the identification of the EGFR-TK inhibiting compound. For this purpose, the cytotoxic effect of a water extract of the fruit of *B. javanica* (BW) and the resulting five fractions after solid-phase extraction (SPE) separation was assessed using the non-small cell lung cancer cell line A549 since these cells overexpress EGFR compared to normal lung cells[9] and were used before.[8] The IC$_{50}$ and standard deviation (s.d.) values for each fraction tested and the relative cell viability are depicted in Figure 1. The aqueous crude extract showed a comparable cytotoxic effect on A549 cells as the ethanolic crude extract studied in our earlier work,[8] with an IC$_{50}$ value of 7.217 μg/mL after incubation of the cells with the aqueous extract for 24 h compared to 19.8 μg/mL after incubation of the cells with the ethanolic extract overnight.[8] These values are also in the same range as earlier published data that reported IC$_{50}$ values between 1.5 and 5.1 μg/mL after incubation of pancreatic cell lines with the ethanolic extract from the fruits of *B. javanica* for 72 h.[10]

The cytotoxic effects of fractions 3 and 4 of the BW were stronger compared to the effect of the crude aqueous extract, revealing IC$_{50}$ values of 0.375 μg/mL for BW3 and 0.439 μg/mL for BW4, respectively. Therefore, these fractions were selected for further investigation to identify their main active constituents.

Compound Identification Using LC/MS and ^{1}H NMR. LC/MS was used to identify the main active constituents of the fractions BW3 and BW4. Figure 2 shows the chromatogram of both fractions in the positive ionization mode. Both fractions presented the same peak at 48.2 min corresponding to a molecular mass of *m/z* 521.22. Although the area under the curve of this peak was similar for both fractions, the BW4 fraction contained other peaks in the chromatogram, indicating that the purity of this fraction was lower than that for fraction

BW3 (86.67% for BW3 and 13.21% for BW4). For this reason, BW3 was selected for further analysis to identify its main constituent.

To elucidate the structure of the compound separated by LC/MS, fraction BW3 was further analyzed using ^{1}H NMR. Figure 3 shows the full ^{1}H NMR spectrum of fraction BW3 and the enlargement of specific regions (5.00–3.90 and 3.00–1.20 ppm), which could be attributed to brusatol, based on existing ^{1}H NMR data.[11] For further verification, the ^{1}H NMR spectra of the fraction were compared to that obtained from a commercial brusatol reference, which revealed the same peaks (see insert in Figure 3). Since these signals had the highest intensity in the BW3 ^{1}H NMR spectrum, it was concluded that brusatol is the main component of this fraction. Brusatol was first identified in extracts of *Brucea sumatrana* in 1967,[12] and it turned out to be one of the two components of *B. javanica* with the highest bioactive potential with regard to anti-cancer effects.[5] Cytotoxic effects of brusatol against cancer cells were first discovered in 1979 for leukemia,[13] and IC$_{50}$ values in the low nM range were demonstrated in many different in vitro cancer cell models by now, as summarized by He et al.[7] Additionally, in vivo studies of xenograft models supported the anti-cancer activity of brusatol with effective dosages varying between 0.5 and 4 mg/kg body weight in mice.[7]

Cytotoxicity and Pro-apoptotic Activity of Brusatol. To demonstrate that brusatol is cytotoxically active, A549 cells were treated with the reference compound to assess the cellular viability. The results demonstrate that brusatol exhibited cytotoxic activity against A549 cells after 24 h incubation (Figure 4), with an IC$_{50}$ value of 0.057 ± 0.002 μg/mL, which corresponds to 109 nM. This result is well in line with earlier studies reporting an IC$_{50}$ value of 28 nM brusatol after treating A549 cells for 72 h[14] or 140 nM[15] and 1.9 μM[16] after an incubation for 24 h.

In addition to the cytotoxic effects of brusatol, its effect on cell apoptosis was determined in A549 cells using a concentration range spanning the IC$_{50}$ value of brusatol's cytotoxic activity. The representative flow cytometry plots in
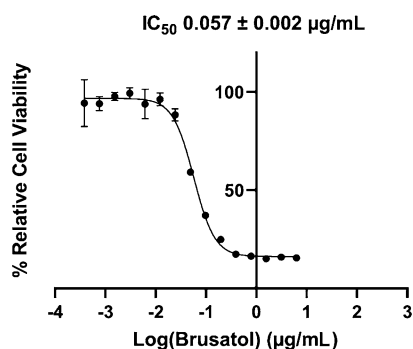
Figure 4. Cytotoxic effect of brusatol on A549 cells. The relative cell viability of brusatol against A549 cancer cells was assessed by MTT assay performed after treatment of A549 cells with brusatol for 24 h and compared to control cells that were treated with solvent control; results are given as mean ± standard deviation, $n = 3$ biological and 3 technical replicates each.

Figure S1 show the proportions of live, necrotic, early apoptotic, and late apoptotic A549 cells after treatment with 10.8−1081 nM brusatol for 24 h. While brusatol did not induce apoptosis at a concentration of 10.8 nM, compared to the untreated cells, the number of total apoptotic cells (early and late) increased about 10-fold after treatment with 108 or 1081 nM brusatol (Figure 5). These results showed that brusatol could induce apoptosis in A549 cells, supporting the cytotoxic effects of brusatol described above.
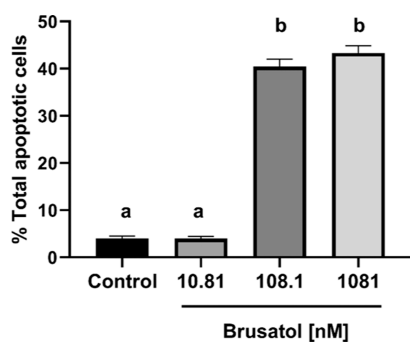
Figure 5. Effect of brusatol on apoptosis in A549 cells. The percentage of total apoptotic cells in relation to the total cell number after treatment with solvent control (control), or with 10.81, 108.1, or 1081 nM brusatol for 24 h is depicted; results are given as mean ± standard deviation, $n = 3$ biological and 3 technical replicates each, statistical comparison was performed by one-way ANOVA with the Holm−Sidak test for multiple comparisons, different letters indicate significant differences.

Besides the cytotoxicity and pro-apoptotic activity of brusatol against cancer cells, also its inhibitory activity against cancer cell migration, invasion, and colony formation has been shown in earlier in vitro studies for diverse cancer cell types.[14,16−22] Furthermore, in vivo experiments demonstrated that the treatment with 1, 2, or 4 mg brusatol per kg body weight reduced tumor growth in various mice xenograft models, for e.g., lung cancer,[11,23] pancreatic cancer,[24,25] colorectal cancer,[20,26,27] melanoma[28] liver cancer,[22,29] breast cancer,[30] leukemia,[31,32] and ovarian cancer.[33] Despite these promising results, studies on the mode of action of brusatol are still inconclusive, as outlined by Cai et al.[34] Several different pathways have been reported so far to be targeted by brusatol,

with the inhibition of Nrf2 as the most evident.[11,19,30] However, it was discussed whether Nrf2 is specifically inhibited or only results from the general inhibition of the translation of short-lived proteins by brusatol.[35,36] Moreover, an inhibitory activity of brusatol on additional cellular pathways has also been described in association with cancer cell cytotoxicity, as, for example, inhibition of STAT3,[16,29,37] PI3K/Akt/ mTOR,[18,22,38,39] RhoA/ROCK,[20] HIF1α,[27,40] and Skp1.[15] However, the potential of brusatol as an EGFR-TK inhibitor has not been examined yet, even though a synergistic effect could be shown when brusatol was used in combination with trastuzumab,[41] erlotinib or gefitinib,[14] which are all TK inhibitors.

EGFR-TK Inhibition Activity of the Crude Extract, Fraction BW3, and Brusatol. To evaluate whether brusatol is the active compound responsible for the inhibitory activity on EGFR-TK by the *B. javanica* extract shown earlier,[8] an enzymatic assay specifically developed for the assessment of EGFR-TK activity[8,42] was used. The inhibitory effects of the crude aqueous extract, fraction BW3, and the brusatol reference compound were analyzed. BW and fraction BW3 inhibited the EGFR-TK activity with IC$_{50}$ values of 289.30 ± 42.19 and 84.33 ± 10.20 μg/mL, respectively (Figure 6a).
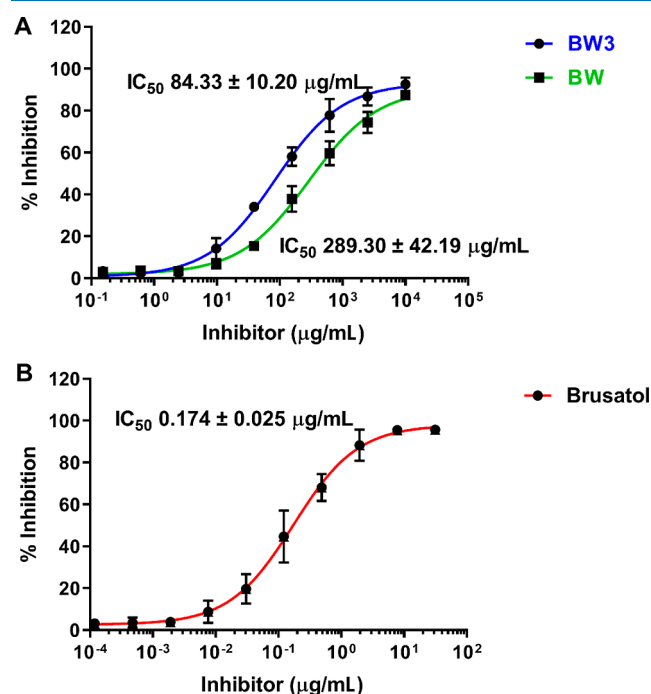
Figure 6. Inhibitory effect of (a) the crude aqueous extract of *B. javanica* (BW) and fraction BW3 and (b) brusatol on EGFR-TK activity compared to the solvent control; results are given as mean ± standard deviation, $n = 3$ biological and 3 technical replicates each.

As hypothesized, brusatol, the main constituent of fraction BW3, showed the highest inhibitory activity against EGFR-TK with an IC$_{50}$ value of 0.174 ± 0.025 μg/mL or 333 nM (Figure 6b). The EGFR-TK inhibition by the brusatol reference compound was about 495 times stronger compared to fraction BW3, which could be explained by the purity of BW3. As visible in the LC/MS chromatogram, this fraction contains other compounds besides brusatol that could potentially inhibit its EGFR-TK inhibitory activity within BW3.

Compared to brusatol, the clinically approved EGFR-TK inhibitors erlotinib and afatinib had lower IC_{50} values of 13.09 and 2.36 nM in this enzymatic assay for EGFR-TK inhibition.[8] Nevertheless, when comparing the cytotoxic effects of brusatol on A549 cells described above (IC_{50} = 109 nM after a 24 h treatment) to those of erlotinib (IC_{50} = 19.4[43] and 25 μM[44] after 24 h, or 2.88[45] and 15.5 μM[46] after 72 h treatment), brusatol showed a better performance, indicating its potential as a candidate for EGFR-TK inhibition in lung cancer cells. Since it is well known that brusatol acts on cancer cell viability via different pathways,[11,15,20,22,27,29] the lower effect in the enzymatic assay and higher effect in the cell-based assay compared to erlotinib could result from simultaneous inhibitory activities of brusatol in addition to EGFR-TK inhibition, as for example Nrf2 inhibition. Through these different inhibitory activities working in parallel, brusatol might have a potential as a multimodal therapeutic for the treatment of EGFR-expressing cancers.

Simulation of the Interaction of Brusatol and EGFR-TK. To further evaluate the specific interaction of brusatol with the EGFR-TK, in silico experiments were performed, aiming to identify the binding site of brusatol on the EGFR-TK. The starting structure of EGFR-TK with brusatol for further investigation on molecular dynamic simulations was selected from the best docking pose. The simulation of the complex was performed for 100 ns for three independent runs. The root-mean-square deviation (RMSD) of the protein backbone is shown in Figure 7a. The RMSD from replicates 1 and 2 equilibrated at ∼0.4 and 0.45 nm, respectively, while for replicate 3, it was at ∼0.25 nm. The RMSD values of the three replicates were stable after 50 ns.

The binding free energies and predicted IC_{50} from the molecular mechanics Poisson−Boltzmann surface area (MM-PBSA) calculations of each run are listed in Table S1, representing the summation of polar, nonpolar, and non-bonded interaction energies. In this part, the results were calculated from 500 snapshots, which were extracted from the stable simulation time in the last 50 ns of each run. The binding free energy (ΔG_{bind}) from replicates 1−3 was −39.806 ± 1.137, −44.426 ± 1.284, and −49.290 ± 0.852, respectively, and brusatol was predicted to bind with EGFR-TK in terms of electrostatic, SASA, and van der Waals interaction energy, with the later contributing the most. On the contrary, polar solvation energy had positive values for this system, indicating that this type of energy did not contribute to the binding of brusatol and EGFR-TK.

For further identification of the key amino acid residues of the binding site, the contribution energies between the residues of the EGFR-TK within a distance of 6 Å of brusatol were calculated. The energy decompositions of the binding residues of this system are presented in Figure 7b. Most of the residues at the binding site had a favorable contribution with negative binding energy values to brusatol, with the highest contribution (<−4 kJ/mol) in LEU694, GLY695, TYR703, and VAL821. In contrast, some amino acid residues were contributing to the system with positive energy, namely, LEU768 and PRO770, and were especially high for the residues ARG817 and ASP831. We found binding free energy contribution of several residues of EGFR-TK with brusatol systems showing the same trend as EGFR-TK in the erlotinib system.[47] The two-dimensional interaction between brusatol and erlotinib with EGFR-TK was visualized using LigPlot[48] and is illustrated in Figure S2. Additionally, a study by
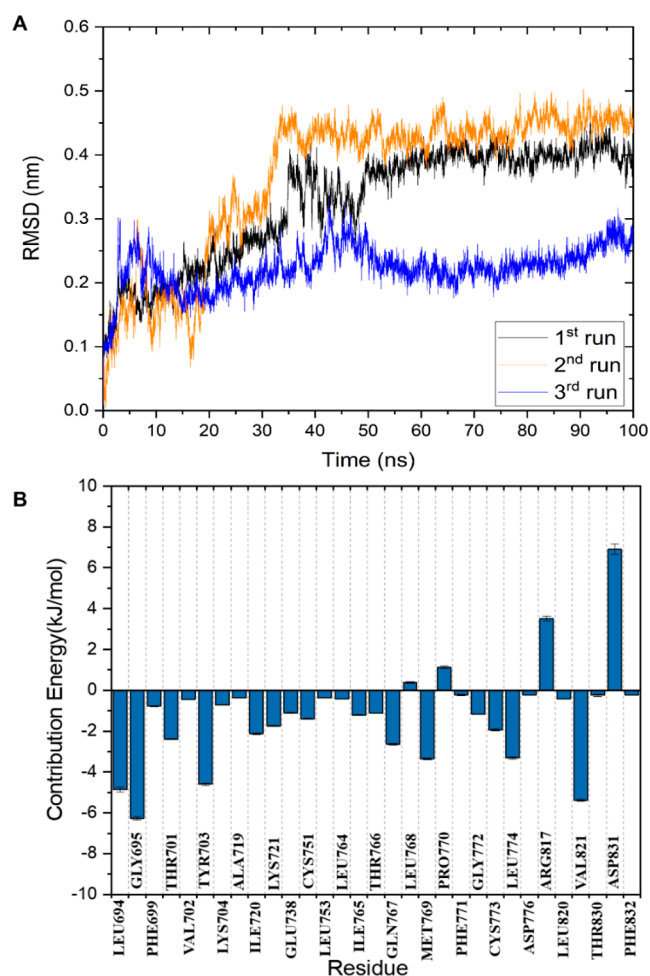
Figure 7. Simulation of the interaction between brusatol and EGFR-TK. (a) Illustration of the stability of the EGFR-TK and brusatol system showing the RMSD calculated in three independent runs of the EGFR-TK backbone over 100 ns and (b) average value of the free contribution energy of each binding residue calculated between 50 and 100 ns.

Tabtimmai et al.[49] demonstrated the interaction between gefitinib with EGFR-TK. Brusatol, erlotinib, and gefitinib shared an H-bond with MET769 and hydrophobic interactions with LEU694, ALA719, LYS721, GLY772, and THR 830. In addition, brusatol formed H-bonds with PRO770, CYS773, LEU820, and ASP831 residues, and VAL702, MET742, THR 766, THR760, LEU768, PHE771, and THR 830 by forming hydrophobic interaction. Furthermore, the brusatol could potentially inhibit double[50] and triple[51] mutant EGFR since the docking score of all structures are similar among them (Table S2). Our computational results showed that brusatol was well docked in the cleft between the N- and C- lobes of EGFR-TK (see Figure 8).

CONCLUSIONS

In this study, brusatol was identified as the key component of the aqueous extract from B. javanica responsible for its EGFR-TK inhibitory activity in a cell-free assay. Moreover, brusatol exhibited cytotoxic and pro-apoptotic effects in A549 lung cancer cells, which express EGFR. In silico experiments identified the binding pocket of brusatol within the intra-cellular TK-domain of the EGFR with the residues of the amino acids LEU694, GLY695, TYR703, and VAL821 of the
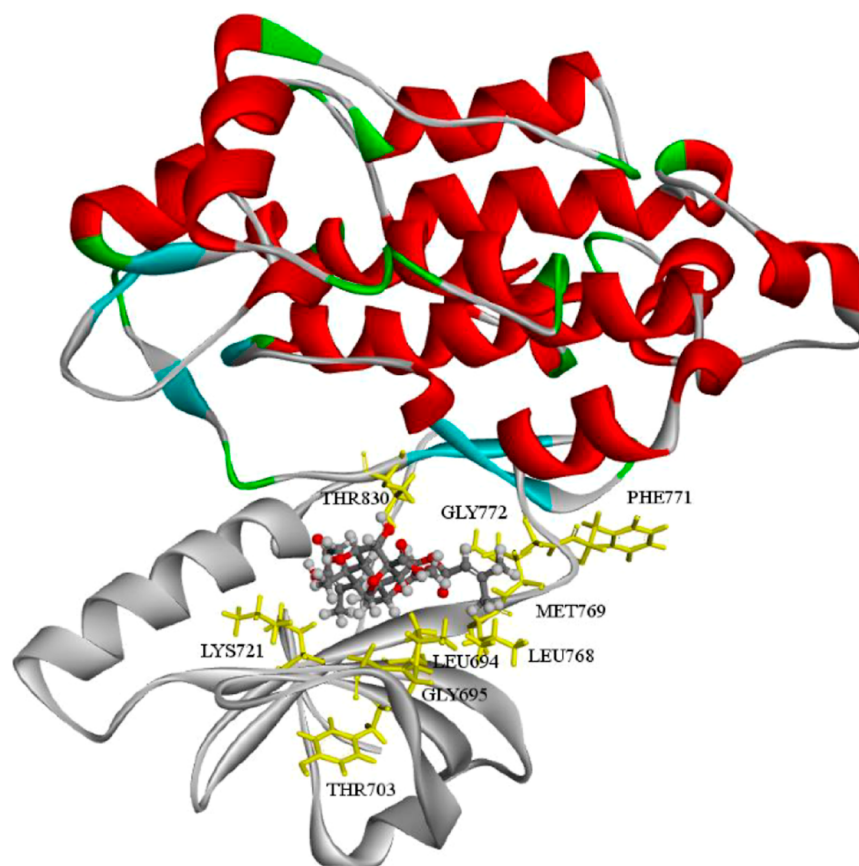
Figure 8. Average structure of EGFR-TK and brusatol complex during 50−100 ns, where brusatol is shown in sticks and balls and binding residues are shown as yellow lines.

EGFR-TK as the most favorable for stably binding brusatol. Therefore, this compound might be useful as a cancer drug as a promising anti-cancer drug with at least dual modes of action, targeting both EGFR-TK and NRF2 inhibition.

◼ MATERIALS AND METHODS

Herbal Extraction and SPE Fractionation. Dried powder of the fruit of *B. javanica* was purchased from the TPC Herb Company, Thailand. The crude water extract of the fruit was prepared by mixing 1 g of dried fruit powder with 9 mL of distilled water for 12 h on a magnetic stirrer. The aqueous extract was filtered through a 11 μm pore size filter, and the water was removed using a rotary evaporator (Rotavapor R-210, Buchi) at 50 °C; finally, the extract was lyophilized overnight (FreeZone, Labconco). The resulting crude extract was weighed and stored for maximum 2 month at 4 °C.

The aqueous-soluble extract (40 mg of the aqueous extract in 1 mL of water) was loaded on a C18 SPE cartridge (Discovery DSC-18 1 mL tubes, 100 mg) to yield five fractions (BW1-5). First, the cartridge was equilibrated with 1 mL of methanol and pre-conditioned with 1 mL of distilled water. The whole extract was loaded and eluted sequentially with the following mixtures of distilled water and methanol: 100:0 (BW1), 80:20 (BW2), 70:30 (BW3), 50:50 (BW4), and 0:100 (BW5), with each having three times the bed volume. The solvent of all collected fractions was evaporated and lyophilized. The dried fractions were stored at 4 °C for a maximum of 2 months until further analysis.

Identification of Compounds Using LC/MS and NMR. To analyze the composition of fractions BW3 and BW4, a microTOF MS (Bruker, Germany) coupled to an Ultimate 3000 LC (Thermo Fischer Scientific, USA) was used. MS measurements were performed in the positive scan mode for a mass range of m/z 500−1000. An injection volume of 20 μL and the analytical column Synergi 4 μm Fusion-RP (150 × 2 mm) were used. Solvent A (0.1% formic acid and 1 g/L ammonium formate in water) and solvent B (0.1% formic acid and 1 g/L ammonium formate in methanol) were used at the following mixing ratios: at minutes 0−30, 100−70% of solvent A and 0−30% of solvent B; at minutes 30−60, 70−0% of solvent A and 30−100% of solvent B; and at minutes 60−65, the final ratio was kept constant. A flow rate of 0.2 mL/min was used, and the column temperature was 40 °C.

^{1}H NMR spectroscopy analysis was conducted to confirm the identification of the main constituent of BW3. First, the sample was dissolved in 600 μL of dimethyl sulfoxide (DMSO)-d_6. ^{1}H NMR data acquisition was performed at 400 MHz using an NMR spectrometer (Avance Bruker). The experiments were run with 64 scans as in previous studies.[11] The relaxation delays and acquisition times allowed for the complete relaxation of the protons; thus, the areas of the signals were proportional to the number of protons that generated them. The ^{1}H NMR spectra were plotted at a fixed value of absolute intensity to be valid for comparative purposes using the MestreNova program (Mestrelab Research, Santiago de Compostela, Spain).

Cell Cultivation. The human lung carcinoma cell line A549 (ATCC-CCL-185) was purchased from the American Type

Culture Collection (ATCC, USA). The cell culture medium and supplements were purchased from Thermo Fisher Scientific (Waltham, MA, USA). The cells were cultured in Dulbecco's modified Eagle medium (DMEM; Gibco, USA) containing 10% fetal bovine serum (Thermo Fisher, USA) and 1% (v/v) penicillin−streptomycin (Sigma-Aldrich, USA) and maintained at 37 °C in a humidified incubator in an atmosphere with 5% CO_2.

Cell Cytotoxicity Assay. The cytotoxic effects of the studied compounds against the A549 cell line were assessed using the MTT assay according to a previously published protocol.[52] 5×10^4 cells/well were seeded in a 96-well plate 24 h prior to the incubation with the test compounds. After incubation for 24 h, the MTT reagent was added for 3 h, and the absorbance was measured at a wavelength of 570 nm and background-corrected by subtracting the absorbance at 630 nm using a microplate reader (TECAN, Switzerland).

Before application of the test compounds in the cell assay, the dried powder was solved in DMSO at a concentration of 100 mg/mL and then further diluted in cell culture medium. To avoid cytotoxic effects, DMSO was used at a maximum concentration of 0.1% when applied to the cells.

Apoptosis Assay. For the apoptosis assay, A549 cells were seeded at a density of 5×10^4 cells/well in 24-well plates and incubated overnight at 37 °C in 5% CO_2. Then, the cells were treated for 24 h with solvent 10.8, 108.1, or 1081 nM brusatol or solvent control diluted in culture medium. After removing the compound-containing medium, the cells were trypsinized. Next, the cell samples were incubated for 20 min at room temperature with the Muse Annexin V & Dead Cell reagent (Merck Millipore Burlington, USA) that uses Annexin V as a marker for apoptosis and 7-aminoactinomycin D as a marker for dead and necrotic cells. After staining with these markers, cells were analyzed according to the manufacturer's instructions by flow cytometry. For analysis, the percentage of viable, early apoptotic, late apoptotic, and necrotic cells in relation to the total number of cells was determined, and the sum of early and late apoptotic cells was used to calculate the percentage of total apoptotic cells.

Kinase Activity Assay. The ADP-Glo kinase assay (Promega, USA) was used to assess the inhibitory activity against EGFR-TK. The experimental process was performed, as described previously.[42]

Computational Analysis. The crystal structure of EGFR-TK was taken from the Protein Data bank, number 1M17,[53] which is the active conformation of the enzyme bound with the FDA-approved drug erlotinib. The molecular docking experiments of the EGFR-TK and brusatol (CID: 73432) complex were carried out using Gold docking programs.[54] The best docking pose of the EGFR-TK and brusatol system was selected using Gromacs 2020.1.[55] A CHARMM36 all-atom force field[55,56] was applied for this simulation. The brusatol topology was generated via the CGenff server (https://cgenff.umaryland.edu/initguess/summary.php#cite_ff). The system was solvated with simple point charge water molecules and neutralized with ion molecules. For energy minimization, the steepest descent algorithm was used until the maximum force was lower than 1000 kJ/mol/nm. For equilibrating the system, two ensembles with a position restraint force of 1000 kJ/mol/nm were applied during each equilibration to all heavy atoms of the protein to allow the free movement of protons, solvent molecules, and ions. The first position restraint NVT ensemble was set at 300 K using a modified Berendsen thermostat[57] for

100 ps, followed by a second position restraint NPT ensemble at 1 bar of pressure using a Parrinello-Rahman barostat[58] for 5 ns. After that, any position restraints were removed from the protein heavy atoms, and a free MD simulation was performed. For MD procedures, hydrogen bond lengths were constrained using the LINCS algorithm[59] allowing for a 2.0 fs time step. A cut-off distance for the short-range neighbor list was set to 1.2 nm for both electrostatic and van der Waals interactions. Long-range electrostatic interactions were approximated using the Particle Mesh Ewald method,[60] and all atomic coordinates were recorded every 10 ps for data collection. Three simulations of 100 ns were performed for this study.

The MM-PBSA is a method to estimate the binding energy between EGFR-TK and brusatol. In this study, the binding interaction and energy contribution per residue were analyzed using g_mmpbs tool.[61]

Statistical Analysis. Where applicable, data are presented as mean ± standard deviation. Three biological (cell passages) and three technical replicates were performed for all in vitro experiments. For the determination of IC_{50} values, statistical analysis was performed with dose−response curves to inhibition [log(inhibitor) vs. a response-variable slope (four parameters) equation in GraphPad Prism Version 8.0.2] (GraphPad Software Inc., USA). For the apoptosis assay, statistical analysis was performed with one-way analysis of variance (ANOVA) with the Holm−Sidak test for multiple comparison. Significant differences were identified at $p < 0.05$.

■ ASSOCIATED CONTENT

ⓢ Supporting Information

The Supporting Information is available free of charge at https://pubs.acs.org/doi/10.1021/acsomega.3c02931.

> Binding free-energy analysis and predicted IC_{50} of EGFR-TK with brusatol, docking score of brusatol with WT, double and triple mutation, effect of brusatol on A549 cell apoptosis, two-dimensional illustrations of EGFR-TK/inhibitor interactions from the docking results of brusatol and erlotinib (PDF)

> Water extract and fractionation; identification of active compound; computational methods; and cytotoxicity, apoptosis, and kinetic activity assays (PDF)

■ AUTHOR INFORMATION

Corresponding Author

> **Kiattawee Choowongkomon** − *Department of Biochemistry, Faculty of Science, Kasetsart University, 10900 Bangkok, Thailand;* ● orcid.org/0000-0002-2421-7859; Phone: +66 85 555 1480; Email: fsciktc@ku.ac.th

Authors

> **Chonticha Suwattanasophon** − *Department of Physiological Chemistry, Faculty of Chemistry, University of Vienna, 1090 Vienna, Austria; Department of Biochemistry, Faculty of Science, Kasetsart University, 10900 Bangkok, Thailand*

> **Agnes Mistlberger-Reiner** − *Department of Physiological Chemistry, Faculty of Chemistry, University of Vienna, 1090 Vienna, Austria;* ● orcid.org/0000-0002-7077-1199

> **Jon Alberdi-Cedeño** − *Department of Physiological Chemistry, Faculty of Chemistry, University of Vienna, 1090 Vienna, Austria; Food Technology, Faculty of Pharmacy, Lascaray Research Center, University of the Basque Country (UPV-EHU), 01006 Vitoria-Gasteiz, Spain*

Marc Pignitter — *Department of Physiological Chemistry, Faculty of Chemistry, University of Vienna, 1090 Vienna, Austria;* ◉ orcid.org/0000-0002-5793-8572

Veronika Somoza — *Department of Physiological Chemistry, Faculty of Chemistry, University of Vienna, 1090 Vienna, Austria; Leibniz-Institute for Food Systems Biology at the Technical University of Munich, 85354 Freising, Germany; Nutritional Systems Biology, Technical University of Munich, 85354 Freising, Germany*

Jürgen König — *Department of Nutritional Sciences, Faculty of Life Sciences, University of Vienna, 1090 Vienna, Austria*

Thomanai Lamtha — *Department of Biochemistry, Faculty of Science, Kasetsart University, 10900 Bangkok, Thailand*

Panatda Wanaragthai — *Interdisciplinary Program of Genetic Engineering and Bioinformatics, Graduate School, Kasetsart University, 10900 Bangkok, Thailand*

Duangnapa Kiriwan — *Interdisciplinary Program of Genetic Engineering and Bioinformatics, Graduate School, Kasetsart University, 10900 Bangkok, Thailand*

Complete contact information is available at:
https://pubs.acs.org/10.1021/acsomega.3c02931

Author Contributions

C.S. and A.M.-R. contributed equally to this work. All authors conceived and designed the experiments, C.S., J.A.C, T.L., and P.W. carried out the experiments. C.S., A.M.R., J.A.C., M.P., and D.K. contributed to the interpretation of the results. C.S. and A.M.R. wrote the manuscript with support from J.A.C. and M.P. Review and editing were carried out by V.S., J.K., and K.C. All authors discussed the results and contributed to the final manuscript. K.C. supervised the project.

Notes

The authors declare no competing financial interest.

■ ABBREVIATIONS

EGFR, epidermal growth factor receptor; EGFR-TK, EGFR tyrosine kinase; IC_{50}, half maximal inhibitory concentration; NSCLC, non-small cell lung cancer; (DMSO)-d_6, dimethyl sulfoxide; DMEM, Dulbecco's modified Eagle's medium

■ REFERENCES

(1) Pottier, C.; Fresnais, M.; Gilon, M.; Jérusalem, G.; Longuespée, R.; Sounni, N. E. Tyrosine kinase inhibitors in cancer: breakthrough and challenges of targeted therapy. *Cancers* **2020**, *12*, 731.

(2) Butler, M. S. Natural products to drugs: natural product-derived compounds in clinical trials. *Nat. Prod. Rep.* **2008**, *25*, 475−516.

(3) Cragg, G. M.; Newman, D. J. Plants as a source of anti-cancer agents. *J. Ethnopharmacol.* **2005**, *100*, 72−79.

(4) Gao, H.; Lamusta, J.; Zhang, W.-F.; Salmonsen, R.; Liu, Y.; O'Connell, E.; Evans, J. E.; Burstein, S.; Chen, J. J. Tumor cell selective cytotoxicity and apoptosis induction by an herbal preparation from Brucea javanica. *N. Am. J. Med. Sci.* **2011**, *4*, 62.

(5) Zhang, J.; Xu, H. X.; Dou, Y. X.; Huang, Q. H.; Xian, Y. F.; Lin, Z. X. Major Constituents From Brucea javanica and Their Pharmacological Actions. *Front. Pharmacol.* **2022**, *13*, 853119.

(6) Chen, J.; Chen, S.; Yang, X.; Wang, S.; Wu, W. Efficacy and safety of Brucea javanica oil emulsion injection as adjuvant therapy for cancer: An overview of systematic reviews and meta-analyses. *Phytomedicine* **2022**, *102*, 154141.

(7) He, T.; Zhou, F.; Su, A.; Zhang, Y.; Xing, Z.; Mi, L.; Li, Z.; Wu, W. Brusatol: A potential sensitizing agent for cancer therapy from Brucea javanica. *Biomed. Pharmacother.* **2023**, *158*, 114134.

(8) Semsri, S.; Seatew, C.; Rattanabunyong, S.; Ruekit, S.; Horata, N.; Panya, A.; Yenchitsomanus, P. T.; Sawatdichaikul, O.; Choowongkomon, K. In-vitro Studies of Anti-EGFR Tyrosine Kinase Activity of Thai nutraceutical Plants. *Iran. J. Pharm. Res.* **2020**, *19*, 199−206.

(9) Zhou, P.; Hu, J.; Wang, X.; Wang, J.; Zhang, Y.; Wang, C. Epidermal growth factor receptor expression affects proliferation and apoptosis in non-small cell lung cancer cells via the extracellular signal-regulated kinase/microRNA 200a signaling pathway. *Oncol. Lett.* **2018**, *15*, 5201−5207.

(10) Lau, S. T.; Lin, Z. X.; Zhao, M.; Leung, P. S. Brucea javanica fruit induces cytotoxicity and apoptosis in pancreatic adenocarcinoma cell lines. *Phytother. Res.* **2008**, *22*, 477−486.

(11) Ren, D.; Villeneuve, N. F.; Jiang, T.; Wu, T.; Lau, A.; Toppin, H. A.; Zhang, D. D. Brusatol enhances the efficacy of chemotherapy by inhibiting the Nrf2-mediated defense mechanism. *Proc. Natl. Acad. Sci. U.S.A.* **2011**, *108*, 1433−1438.

(12) Sim, K. Y.; Sims, J. J.; Geissman, T. A. Constituents of Brucea sumatrana. I. Brusatol. *J. Org. Chem.* **1968**, *33*, 429−431.

(13) Hall, I. H.; Lee, K. H.; Elgebaly, S.; Imakura, Y.; Sumida, Y.; Wu, R. Y. Antitumor Agents XXXIV: Mechanism of Action of Bruceoside a and Brusatol on Nucleic Acid Metabolism of P388 Lymphocytic Leukemia Cells. *J. Pharm. Sci.* **1979**, *68*, 883−887.

(14) Xie, J.; Lai, Z.; Zheng, X.; Liao, H.; Xian, Y.; Li, Q.; Wu, J.; Ip, S.; Xie, Y.; Chen, J.; Su, Z.; Lin, Z.; Yang, X. Apoptotic activities of brusatol in human non-small cell lung cancer cells: Involvement of ROS-mediated mitochondrial-dependent pathway and inhibition of Nrf2-mediated antioxidant response. *Toxicology* **2021**, *451*, 152680.

(15) Xing, S.; Nong, F.; Wang, Y.; Huang, D.; Qin, J.; Chen, Y. F.; He, D. H.; Wu, P. E.; Huang, H.; Zhan, R.; Xu, H.; Liu, Y. Q. Brusatol has therapeutic efficacy in non-small cell lung cancer by targeting Skp1 to inhibit cancer growth and metastasis. *Pharmacol. Res.* **2022**, *176*, 106059.

(16) Zhou, J.; Hou, J.; Wang, J.; Wang, J.; Gao, J.; Bai, Y. Brusatol inhibits laryngeal cancer cell proliferation and metastasis via abrogating JAK2/STAT3 signaling mediated epithelial-mesenchymal transition. *Life Sci.* **2021**, *284*, 119907.

(17) Chandrasekaran, J.; Balasubramaniam, J.; Sellamuthu, A.; Ravi, A. An in vitro study on the reversal of epithelial to mesenchymal transition by brusatol and its synergistic properties in triple-negative breast cancer cells. *J. Pharm. Pharmacol.* **2021**, *73*, 749−757.

(18) Chen, Z.; He, B.; Zhao, J.; Li, J.; Zhu, Y.; Li, L.; Bao, W.; Zheng, J.; Yu, H.; Chen, G. Brusatol suppresses the growth of intrahepatic cholangiocarcinoma by PI3K/Akt pathway. *Phytomedicine* **2022**, *104*, 154323.

(19) Ko, E.; Kim, D.; Min, D. W.; Kwon, S. H.; Lee, J. Y. Nrf2 regulates cell motility through RhoA-ROCK1 signalling in non-small-cell lung cancer cells. *Sci. Rep.* **2021**, *11*, 1247.

(20) Lu, R. J.; Zhao, G. Z.; Jiang, R.; He, S.; Xu, H.; He, J. M.; Sun, Y.; Wu, M. N.; Ran, J. H.; Chen, D. L.; Li, J. Brusatol Inhibits Proliferation and Metastasis of Colorectal Cancer by Targeting and Reversing the RhoA/ROCK1 Pathway. *BioMed Res. Int.* **2022**, *2022*, 7132159.

(21) Wang, T.; Chen, Z.; Chen, H.; Yu, X.; Wang, L.; Liu, X. Brusatol inhibits the growth of renal cell carcinoma by regulating the PTEN/PI3K/AKT pathway. *J. Ethnopharmacol.* **2022**, *288*, 115020.

(22) Ye, R.; Dai, N.; He, Q.; Guo, P.; Xiang, Y.; Zhang, Q.; Hong, Z.; Zhang, Q. Comprehensive anti-tumor effect of Brusatol through inhibition of cell viability and promotion of apoptosis caused by autophagy via the PI3K/Akt/mTOR pathway in hepatocellular carcinoma. *Biomed. Pharmacother.* **2018**, *105*, 962−973.

(23) Park, S. H.; Kim, J. H.; Ko, E.; Kim, J. Y.; Park, M. J.; Kim, M. J.; Seo, H.; Li, S.; Lee, J. Y. Resistance to gefitinib and cross-resistance to irreversible EGFR-TKIs mediated by disruption of the Keap1-Nrf2 pathway in human lung cancer cells. *FASEB J.* **2018**, *32*, 5862−5873.

(24) Lu, Z.; Lai, Z. Q.; Leung, A. W. N.; Leung, P. S.; Li, Z. S.; Lin, Z. X. Exploring brusatol as a new anti-pancreatic cancer adjuvant: biological evaluation and mechanistic studies. *Oncotarget* **2017**, *8*, 84974−84985.

(25) Xiang, Y.; Ye, W.; Huang, C.; Yu, D.; Chen, H.; Deng, T.; Zhang, F.; Lou, B.; Zhang, J.; Shi, K.; Chen, B.; Zhou, M. Brusatol Enhances the Chemotherapy Efficacy of Gemcitabine in Pancreatic Cancer via the Nrf2 Signalling Pathway. *Oxid. Med. Cell. Longev.* **2018**, *2018*, 2360427.

(26) Evans, J. P.; Winiarski, B. K.; Sutton, P. A.; Jones, R. P.; Ressel, L.; Duckworth, C. A.; Pritchard, D. M.; Lin, Z. X.; Fretwell, V. L.; Tweedle, E. M.; Costello, E.; Goldring, C. E.; Copple, I. M.; Park, B. K.; Palmer, D. H.; Kitteringham, N. R. The Nrf2 inhibitor brusatol is a potent antitumour agent in an orthotopic mouse model of colorectal cancer. *Oncotarget* **2018**, *9*, 27104−27116.

(27) Oh, E. T.; Kim, C. W.; Kim, H. G.; Lee, J. S.; Park, H. J. Brusatol-Mediated Inhibition of c-Myc Increases HIF-1α Degradation and Causes Cell Death in Colorectal Cancer under Hypoxia. *Theranostics* **2017**, *7*, 3415−3431.

(28) Wang, M.; Shi, G.; Bian, C.; Nisar, M. F.; Guo, Y.; Wu, Y.; Li, W.; Huang, X.; Jiang, X.; Bartsch, J. W.; Ji, P.; Zhong, J. L. UVA Irradiation Enhances Brusatol-Mediated Inhibition of Melanoma Growth by Downregulation of the Nrf2-Mediated Antioxidant Response. *Oxid. Med. Cell. Longev.* **2018**, *2018*, 9742154.

(29) Lee, J. H.; Mohan, C. D.; Deivasigamani, A.; Jung, Y. Y.; Rangappa, S.; Basappa, S.; Chinnathambi, A.; Alahmadi, T. A.; Alharbi, S. A.; Garg, M.; Lin, Z. X.; Rangappa, K. S.; Sethi, G.; Hui, K. M.; Ahn, K. S. Brusatol suppresses STAT3-driven metastasis by downregulating epithelial-mesenchymal transition in hepatocellular carcinoma. *J. Adv. Res.* **2020**, *26*, 83−94.

(30) Bovilla, V. R.; Kuruburu, M. G.; Bettada, V. G.; Krishnamurthy, J.; Sukocheva, O. A.; Thimmulappa, R. K.; Shivananju, N. S.; Balakrishna, J. P.; Madhunapantula, S. V. Targeted Inhibition of Anti-Inflammatory Regulator Nrf2 Results in Breast Cancer Retardation In Vitro and In Vivo. *Biomedicines* **2021**, *9*, 1119.

(31) Cheng, C.; Yuan, F.; Chen, X. P.; Zhang, W.; Zhao, X. L.; Jiang, Z. P.; Zhou, H. H.; Zhou, G.; Cao, S. Inhibition of Nrf2-mediated glucose metabolism by brusatol synergistically sensitizes acute myeloid leukemia to Ara-C. *Biomed. Pharmacother.* **2021**, *142*, 111652.

(32) Kannan, S.; Irwin, M. E.; Herbrich, S. M.; Cheng, T.; Patterson, L. L.; Aitken, M. J. L.; Bhalla, K.; You, M. J.; Konopleva, M.; Zweidler-McKay, P. A.; Chandra, J. Targeting the NRF2/HO-1 Antioxidant Pathway in FLT3-ITD-Positive AML Enhances Therapy Efficacy. *Antioxidants* **2022**, *11*, 717.

(33) Tian, Z.; Yang, Y.; Wu, H.; Chen, Y.; Jia, H.; Zhu, L.; He, R.; Jin, Y.; Zhou, B.; Ge, C.; Sun, Y.; Yang, Y. The Nrf2 inhibitor brusatol synergistically enhances the cytotoxic effect of lapatinib in HER2-positive cancers. *Heliyon* **2022**, *8*, No. e10410.

(34) Cai, S. J.; Liu, Y.; Han, S.; Yang, C. Brusatol, an NRF2 inhibitor for future cancer therapeutic. *Cell Biosci.* **2019**, *9*, 45.

(35) Harder, B.; Tian, W.; La Clair, J. J.; Tan, A. C.; Ooi, A.; Chapman, E.; Zhang, D. D. Brusatol overcomes chemoresistance through inhibition of protein translation. *Mol. Carcinog.* **2017**, *56*, 1493−1500.

(36) Vartanian, S.; Ma, T. P.; Lee, J.; Haverty, P. M.; Kirkpatrick, D. S.; Yu, K.; Stokoe, D. Application of Mass Spectrometry Profiling to Establish Brusatol as an Inhibitor of Global Protein Synthesis. *Mol. Cell. Proteomics* **2016**, *15*, 1220−1231.

(37) Lee, J. H.; Rangappa, S.; Mohan, C. D.; Basappa; Sethi, G.; Lin, Z. X.; Rangappa, K. S.; Ahn, K. S. Brusatol, a Nrf2 Inhibitor Targets STAT3 Signaling Cascade in Head and Neck Squamous Cell Carcinoma. *Biomolecules* **2019**, *9*, 550.

(38) Guo, S.; Zhang, J.; Wei, C.; Lu, Z.; Cai, R.; Pan, D.; Zhang, H.; Liang, B.; Zhang, Z. Anticancer effects of brusatol in nasopharyngeal carcinoma through suppression of the Akt/mTOR signaling pathway. *Cancer Chemother. Pharmacol.* **2020**, *85*, 1097−1108.

(39) Pei, Y.; Hwang, N.; Lang, F.; Zhou, L.; Wong, J. H.; Singh, R. K.; Jha, H. C.; El-Deiry, W. S.; Du, Y.; Robertson, E. S. Quassinoid analogs with enhanced efficacy for treatment of hematologic malignancies target the PI3Kγ isoform. *Commun. Biol.* **2020**, *3*, 267.

(40) Lu, Y.; Wang, B.; Shi, Q.; Wang, X.; Wang, D.; Zhu, L. Brusatol inhibits HIF-1 signaling pathway and suppresses glucose uptake under hypoxic conditions in HCT116 cells. *Sci. Rep.* **2016**, *6*, 39123.

(41) Yang, Y.; Tian, Z.; Guo, R.; Ren, F. Nrf2 Inhibitor, Brusatol in Combination with Trastuzumab Exerts Synergistic Antitumor Activity in HER2-Positive Cancers by Inhibiting Nrf2/HO-1 and HER2-AKT/ERK1/2 Pathways. *Oxid. Med. Cell. Longev.* **2020**, *2020*, 9867595.

(42) Seetaha, S.; Ratanabanyong, S.; Choowongkomon, K. Expression, purification, and characterization of the native intra-cellular domain of human epidermal growth factor receptors 1 and 2 in Escherichia coli. *Appl. Microbiol. Biotechnol.* **2019**, *103*, 8427−8438.

(43) Sever, B.; Altintop, M. D.; Ozdemir, A.; Akalin Ciftci, G.; Ellakwa, D. E.; Tateishi, H.; Radwan, M. O.; Ibrahim, M. A. A.; Otsuka, M.; Fujita, M.; Ciftci, H. I.; Ali, T. F. S. In Vitro and In Silico Evaluation of Anticancer Activity of New Indole-Based 1,3,4-Oxadiazoles as EGFR and COX-2 Inhibitors. *Molecules* **2020**, *25*, 5190.

(44) Kritikou, I.; Giannopoulou, E.; Koutras, A. K.; Labropoulou, V. T.; Kalofonos, H. P. The combination of antitumor drugs, exemestane and erlotinib, induced resistance mechanism in H358 and A549 non-small cell lung cancer (NSCLC) cell lines. *Pharm. Biol.* **2013**, *52*, 444−452.

(45) Van Der Steen, N.; Potze, L.; Giovannetti, E.; Cavazzoni, A.; Ruijtenbeek, R.; Rolfo, C.; Pauwels, P.; Peters, G. J. Molecular mechanism underlying the pharmacological interactions of the protein kinase C-beta inhibitor enzastaurin and erlotinib in non-small cell lung cancer cells. *Am. J. Cancer Res.* **2017**, *7*, 816−830.

(46) Zhao, J.; Kelnar, K.; Bader, A. G. In-depth analysis shows synergy between erlotinib and miR-34a. *PLoS One* **2014**, *9*, No. e89105.

(47) Kiriwan, D.; Seetaha, S.; Jiwacharoenchai, N.; Tabtimmai, L.; Sousa, S. F.; Songtawee, N.; Choowongkomon, K. Identification of tripeptides against tyrosine kinase domain of EGFR for lung cancer cell inhibition by in silico and in vitro studies. *Chem. Biol. Drug Des.* **2022**, *99*, 456−469.

(48) Laskowski, R. A.; Swindells, M. B. *LigPlot+: Multiple Ligand−Protein Interaction Diagrams for Drug Discovery*; ACS Publications, 2011.

(49) Tabtimmai, L.; Supakun, P.; Toviwek, B.; Jiwacharoenchai, N.; Kiriwan, D.; Aiebchun, T.; Gleeson, M. P.; Choowongkomon, K. 4-Aryl-N-phenylpyrimidin-2-amines targeting EGFR-tyrosine kinase attenuated EGFR-expressing cell lines. *Eur. J. Med. Chem. Rep.* **2022**, *5*, 100062.

(50) Hoogenboom, N.; Demont, D.; de Zwart, E.; Verkaik, S.; Emmelot, M.; van de Kar, B.; Kaptein, A.; Barf, T. Discovery and optimization of covalent EGFR T790M/L858R mutant inhibitors. *Bioorg. Med. Chem. Lett.* **2021**, *52*, 128406.

(51) Kashima, K.; Kawauchi, H.; Tanimura, H.; Tachibana, Y.; Chiba, T.; Torizawa, T.; Sakamoto, H. CH7233163 overcomes osimertinib-resistant EGFR-Del19/T790M/C797S mutation. *Mol. Cancer Therapeut.* **2020**, *19*, 2288−2297.

(52) Obounchoey, P.; Tabtimmai, L.; Suphakun, P.; Thongkhao, K.; Eurtivong, C.; Gleeson, M. P.; Choowongkomon, K. In silico identification and in vitro validation of nogalamycin N-oxide

(NSC116555) as a potent anticancer compound against non−small cell lung cancer cells. *J. Cell. Biochem.* **2019**, *120*, 3353−3361.

(53) Stamos, J.; Sliwkowski, M. X.; Eigenbrot, C. Structure of the epidermal growth factor receptor kinase domain alone and in complex with a 4-anilinoquinazoline inhibitor. *J. Biol. Chem.* **2002**, *277*, 46265−46272.

(54) Cole, J.; Nissink, J.; Taylor, R. Protein-ligand docking and virtual screening with GOLD. *Virtual Screening in Drug Discovery*; Taylor & Francis CRC Press Boca Raton, 2005; Vol. *1*, pp 379−415.

(55) Abraham, M. J.; Murtola, T.; Schulz, R.; Páll, S.; Smith, J. C.; Hess, B.; Lindahl, E. GROMACS: High performance molecular simulations through multi-level parallelism from laptops to super-computers. *SoftwareX* **2015**, *1−2*, 19−25.

(56) Vanommeslaeghe, K.; Hatcher, E.; Acharya, C.; Kundu, S.; Zhong, S.; Shim, J.; Darian, E.; Guvench, O.; Lopes, P.; Vorobyov, I. CHARMM general force field: A force field for drug like molecules compatible with the CHARMM all atom additive biological force fields. *J. Comput. Chem.* **2010**, *31*, 671−690.

(57) Bussi, G.; Donadio, D.; Parrinello, M. Canonical sampling through velocity rescaling. *J. Chem. Phys.* **2007**, *126*, 014101.

(58) Nosé, S.; Klein, M. Constant pressure molecular dynamics for molecular systems. *Mol. Phys.* **1983**, *50*, 1055−1076.

(59) Hess, B.; Bekker, H.; Berendsen, H. J.; Fraaije, J. G. LINCS: A linear constraint solver for molecular simulations. *J. Comput. Chem.* **1997**, *18*, 1463−1472.

(60) Darden, T.; York, D.; Pedersen, L. Particle mesh Ewald: An N log (N) method for Ewald sums in large systems. *J. Chem. Phys.* **1993**, *98*, 10089−10092.

(61) Kumari, R.; Kumar, R.; Lynn, A.; Lynn, A. g_mmpbsa A GROMACS tool for high-throughput MM-PBSA calculations. *J. Chem. Inf. Model.* **2014**, *54*, 1951−1962.